ORIGINAL ARTICLE

Fabrication and Cell Behavior Assessment of Antibacterial Micro/nano-patterned Chitosan Films

Erika NISHIDA[1], Hirofumi MIYAJI[1], Tsutomu SUGAYA[1], and Tsukasa AKASAKA[2]

[1]Department of Periodontology and Endodontology, Faculty of Dental Medicine, Hokkaido University, Sapporo, Japan
[2] Department of Biomaterials and Bioengineering, Faculty of Dental Medicine, Hokkaido University, Sapporo, Japan

Synopsis
The surface of biomaterials with a fine micro/nano-pattern reportedly affects cell behavior. Chitosan was previously shown to exhibit antibacterial properties and thus here we evaluated the cellular response and antibacterial activity of chitosan micro/nano patterns prepared by the imprint method. We fabricated micro/nano patterns with different sizes and shapes of pillars, grooves, and holes. The chitosan pattern films exhibited antibacterial activity towards *Streptococcus mutans*. In addition, we observed mammalian cells adhering to and spreading on the chitosan pattern, and found that the orientation of the cells was controlled by the shape of the pattern.

Key words: *biomaterial surfaces, chitosan, Streptococcus mutans, MC3T3-E1 cell*

Introduction

Biomaterial surfaces covered with micro/nano-patterns affect the responses of adsorbed biological materials [1,2]. Micro/nano-patterned substrates significantly increase the total surface area, the wettability, and protein adsorption properties of biomaterials [3], and influence cell behavior such as adhesion, differentiation and proliferation [4-6]. Micro/nano-patterned biomaterials are used clinically in drug delivery systems and medical implants [7-8].

Biomaterials should exhibit antibacterial properties to decrease the risk of infection. Chitosan is a polymer easily obtained by the deacetylation of chitin and shows low toxicity. It is primarily used to form fibers and in food. Chitosan-based biomaterials exhibit hydrophilic properties and up-regulate cell adhesion, proliferation and differentiation [9-11]. In addition, chitosan is biodegradable, shows hemostatic effects, bone conduction, and acts as a drug carrier [12-15]. The cationic action of protonated amino groups (NH_3^+) in chitosan interacts with negatively charged bacterial cell membranes [16]. These amino groups form a physical barrier preventing the uptake of nutrients into the cell [17,18]. Cationic amino groups reduce the osmotic stability of bacterial cells and cause leakage of intracellular components, resulting in high antimicrobial activity [19,20]. Therefore, micro/nano patterns formed with chitosan could be candidate biomaterials with antibacterial activity.

Previous studies have shown that chitosan membranes with micropatterns on the substrate surface generated by femtosecond laser microfabrication reduce bacterial adhesion. Biomaterial applications require further detailed study of the relationship between chitosan-based micro/nano-pattern configurations and cellular responses. Here, we prepared chitosan micro/nano-patterned (grooves, pillars, and holes) films using the imprint method and examined bacterial and mammalian cell behavior on the surfaces.

Materials and methods

1. Preparation of silicone replica molds

Silicone rubber replica molds were prepared according to methods previously reported [21,22]. Briefly, silicon master molds (Kyodo International Inc., Kawasaki, Japan) were patterned at 14 areas, each 5 × 5 mm^2. The patterns were grooves (the widths of the ridges and grooves were 2 μm, 1 μm, or 500 nm), holes (both pitch and diameter were 2 μm, 1 μm, or 500 nm), and pillars (both pitch and diameter were 2 μm, 1 μm, or 500 nm) at a height or depth of 2 μm or 500 nm. Resin replicas were prepared by curing photo-curable resin (PAK-01, Toyo Gosei Co., Ltd., Tokyo, Japan) with the silicon master mold using a UV nanoimprinter (EUN-4200, Engineering System Co., Ltd., Nagano, Japan) at a pressure of 0.4 MPa for 10 min. Next, polydimethylsiloxane (PDMS) prepolymer (KE-106 and CAT-RG, 10:1 mix; Shin-Etsu Chemical, Tokyo, Japan) was cast against the above-mentioned replica mold [23]. The prepolymer was then heat-cured at 60°C for 3 days, and then at 100°C for 1 day. Peeling off the cured polymer provided the PDMS replica mold.

2. Preparation of chitosan patterns

To prepare a chitosan micro/nano-patterned surface, chitosan (Chitosan 500, degree of acetylation: 88%, Mw: 51.4 x 10^4 Da, FUJIFILM Wako Pure Chemical Corporation, Ltd., Osaka, Japan) was dissolved at a concentration of 2 wt% in 2.5% acetic acid. Insoluble residues were removed by filtration through a 0.22 μm polyethersulfone filter (AGC Techno Glass Co., Ltd., Shizuoka, Japan). The chitosan solution was poured at 0.45 mL/cm^2 on the patterned silicone mold surrounded by an acrylic frame, then degassed and dried at 80°C. The chitosan film was peeled off carefully and thermally crosslinked at 150°C for 3 h. The resulting film was swelled in phosphate-buffered saline (PBS: 20 mM K_2HPO_4/KH_2PO_4, 150 mM NaCl, pH 7.4) for 3 h in a cell culture dish or on a plastic film. After removing the PBS, the swelled chitosan films were dried and fixed to a substrate to use in the following assays.

3. Characterization of the surface of chitosan patterns

The chitosan pattern was coated with Pt-Pd using a sputtering apparatus (E-1030; Hitachi High-Tech Fielding Corp., Tokyo, Japan). The surface morphology of the patterns was observed using scanning electron microscopy (SEM) (S-4000; Hitachi High-Tech Fielding Corp.).

4. Bacterial attachment and viability assay

The facultative anaerobe *Streptococcus mutans* ATCC 35668 was grown aerobically in brain heart infusion (BHI) broth (Pearlcore®, Eiken Chemical Co. Ltd., Tokyo, Japan) at 37°C for several days. The bacteria were harvested by centrifugation at 2,500 × *g* (Kubota Centrifuge 2700; KUBOTA, Tokyo, Japan), washed in PBS, and suspended in the same buffer to an optical density (OD) of 0.5 at 650 nm.

To estimate bacterial attachment, each chitosan patterned film was placed vertically in BHI medium containing 1% sucrose (FUJIFILM Wako Pure Chemical Corporation, Ltd.) in a cell culture dish, then a suspension of *S. mutans* at a final concentration of 2.1×10^8 colony-forming units [CFU]/mL was added. The samples were incubated aerobically at 37°C for 2 h. The morphology and number of attached bacteria were determined by washing the patterns with PBS twice and immersing in a fixative (2% glutaraldehyde in PBS) for 2 h. The samples were dehydrated in graded ethanol (50%, 60%, 70%, 80%, 90%, 95%, 99.5%, and 100%) and dried with CO_2 in a critical point dryer (Hitachi HCP-1). The bacteria were coated by sputtering with Pt-Pd using a coater and examined by SEM. The number of attached bacteria was counted from 9 different random fields (62.5 × 78.7 μm^2/field) for each pattern from the SEM images [21]. The results are presented as mean ± standard deviation (SD) of three experiments.

The area of each colony formed on the patterns was measured by placing the samples vertically in BHI medium and incubating aerobically at a final bacterial concentration of 5.3×10^9 CFU/mL at 37°C for 5 days. Polyethyleneterephthalate film (PET, 0.5-mm-thick PG-1; Acrysunday Co., Ltd., Tokyo, Japan) and a micro cover glass (18 × 18 mm, thickness No. 1, Matsunami Glass Ind., Ltd., Osaka, Japan) were used as control substrates. The area of colony formation was observed and measured by SEM by treating the specimens as described above for SEM. The area of each colony was measured from 9 different random fields (3.12 × 3.94 mm^2/field) for each pattern from the SEM images [21]. The results are presented as mean ± standard deviation (SD) of three experiments.

The LIVE/DEAD bacterial viability assay [24,25] was conducted by spotting 10 μL of a 2.1×10^8 CFU/mL bacterial suspension on each

specimen, covering with a plastic film, and incubating aerobically at 37°C for 1 h. The specimens were washed twice with PBS to remove non-adhered cells, then stained with an equal volume of the dye mixture in a LIVE/DEAD *Bac*Light bacterial viability kit (L13152, Molecular Probes, Thermo Fisher Scientific, Waltham, MA, USA) and BHI medium, according to the manufacturer's instructions. The specimens were incubated in the dark for 15 min at room temperature. After rinsing gently with PBS, *S. mutans* was observed using a fluorescence microscope (BIOREVO BZ-9000, Keyence, Osaka, Japan). The stained bacteria were monitored for both green emission (470/525 nm) for active bacteria and red emission (545/605 nm) for inactive bacteria.

5. MC3T3-E1 cell attachment assay

The ability of mammalian cells to attach to the formed patterns was determined using mouse osteoblastic MC3T3-E1 cells (RIKEN Bioresource Center, Tsukuba, Japan). MC3T3-E1 cells (3×10^4) were seeded on each pattern and cultured in humidified 5% CO_2 at 37°C using medium (MEM alpha-GlutaMAX-I, Thermo Fisher Scientific) supplemented with 10% fetal bovine serum (FBS; Thermo Fisher Scientific) and 1% antibiotics (Pen Strep, Thermo Fisher Scientific). After 2 h of culture, the samples were fixed with 2.5% glutaraldehyde in 0.1 M sodium cacodylate buffer (pH 7.4) for 30 min and rinsed with PBS. After Giemsa staining, the adherent cells were observed with an optical microscope, and the cell adhesion rate (number of spread cells/total number of adherent cells) in each pattern was measured. Also, after 24 h of culture, the samples were fixed with 2.5% glutaraldehyde in 0.1 M sodium cacodylate buffer (pH 7.4) for 30 min and rinsed in cacodylate buffer solution, then the patterns were dehydrated in increasing concentrations of ethanol. Following critical point drying, the morphology of the attached cells on the patterns was analyzed by SEM at an accelerating voltage of 10 kV after coating with a thin layer of Pt–Pd.

Results and Discussion

1. Preparation of chitosan patterns

We attempted to pattern chitosan using a combination of micro/nano-molding and thermal crosslinking, as shown in Fig. 1. It was easy to

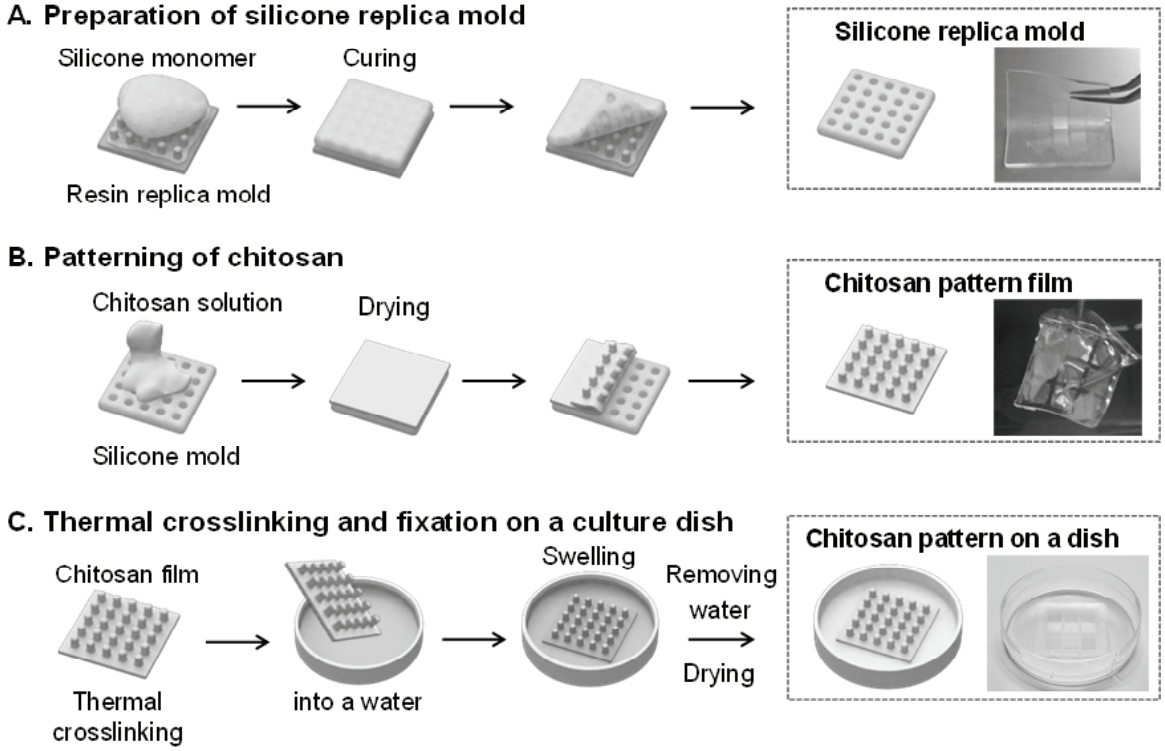

Figure 1
Procedure for chitosan patterning via micro-molding and thermal crosslinking. (A) Preparation of the silicone replica mold, (B) patterning of chitosan, and (C) thermal crosslinking and fixation on a culture dish.

mold a 2 wt% chitosan solution by drying, because of its low viscosity, and then form strong films. The final process for strengthening chitosan film typically involves a conventional insolubilization process by neutralization with NaOH [26-28]. It was previously reported that the antibacterial activity of un-neutralized chitosan films is stronger than that of neutralized chitosan films [29]. Thus, here we instead used thermal crosslinking to insolubilize the chitosan patterns and form films that exhibit high anti-bacterial activity due to their amino acetate groups. However, the disadvantage of thermal crosslinking is that the chitosan patterns are damaged, depending on the degree of crosslinking, temperature, and time. The chitosan films turned brown or dark brown and thus here we crosslinked the samples at 150°C for 3 h to provide adequate stability and minimize damage. The chitosan patterns were sufficiently stable for biological assays.

SEM images of the surfaces of the resulting chitosan patterns are shown in Fig. 2. The top row shows groove and hole patterns 2 μm in diameter and 2 μm in height, and pillars 2 μm, 1 μm, and 500 nm in diameter and 2 μm in height. The middle and lower rows show patterns 500 nm in height and planar chitosan. The pattern shapes were easily obtained by transfer from the corresponding mold. Shapes of small (500 nm)

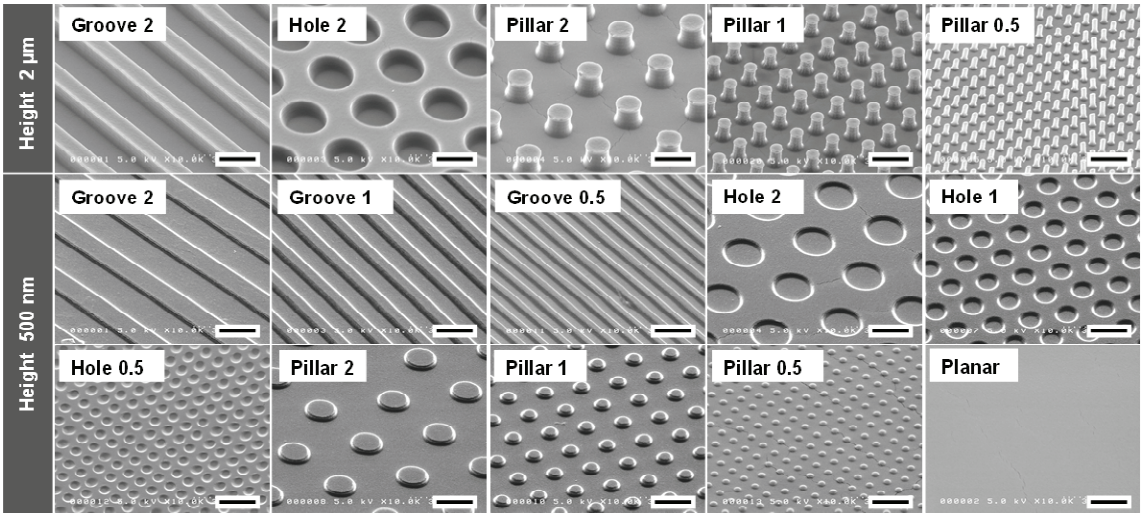

Figure 2
SEM images of the surface of chitosan patterns at a 45°tilt. (Upper row) chitosan grooves, holes, and pillars 2 μm in height. (Middle and lower rows) chitosan grooves, holes, and pillars 500 nm in height. Scale bar indicates 2 μm.

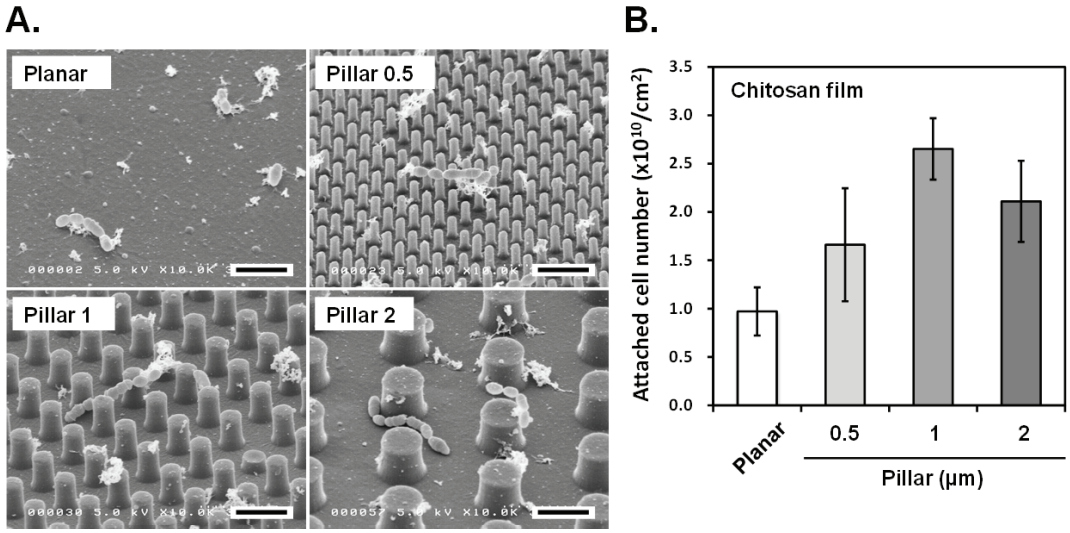

Figure 3
(A) SEM images of *Streptococcus mutans* attached on planar chitosan or chitosan pillars 500 nm, 1 μm, or 2 μm in diameter and 2 μm in height. The cells were incubated on the patterns for 1 h. Scale bars indicate 2 μm. (B) Bar graph of the number of attached *S. mutans* cells on the planar chitosan or chitosan pillars 500 nm, 1 μm, or 2 μm in diameter and 2 μm in height.

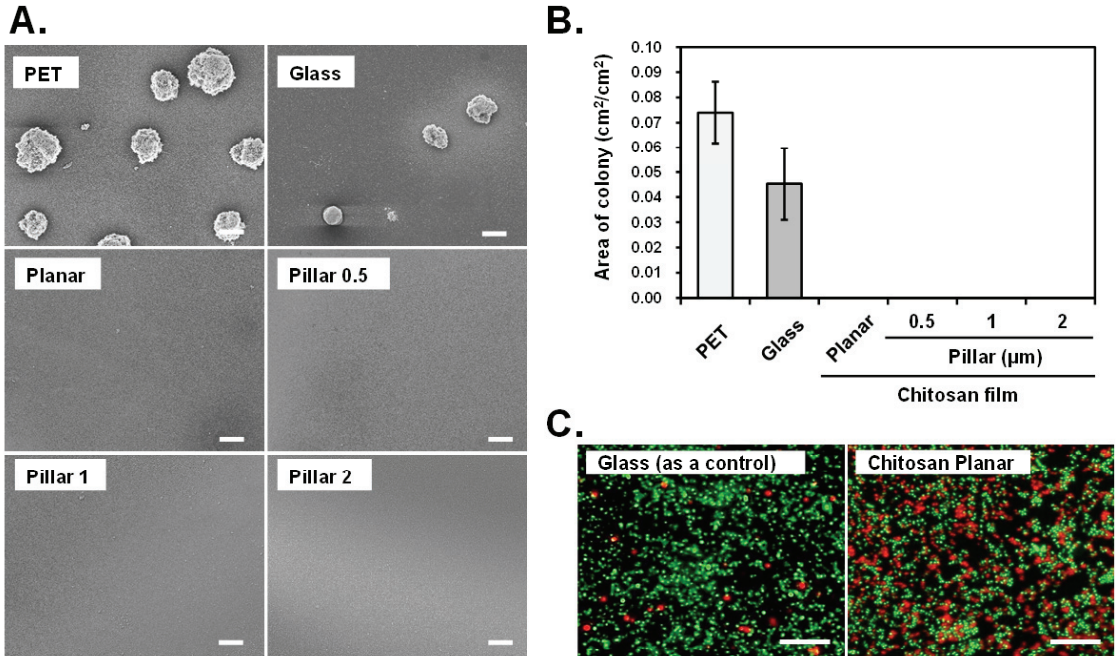

Figure 4
(A) SEM images of *S. mutans* colonies. The cells were incubated on polyethyleneterephthalate (PET) film, cover glass, planar chitosan, or chitosan pillars 500 nm, 1 μm, or 2 μm in diameter and 2 μm in height for 5 days. Scale bars indicate 100 μm. (B) Bar graph of the area of colonies on the samples after 5 days' incubation. (C) Fluorescence microscopy images of LIVE/DEAD bacterial viability assays of *S. mutans* on (Left) a cover glass as a control or (Right) planar chitosan. The cells were incubated on the samples for 1 h. Scale bars indicate 10 μm.

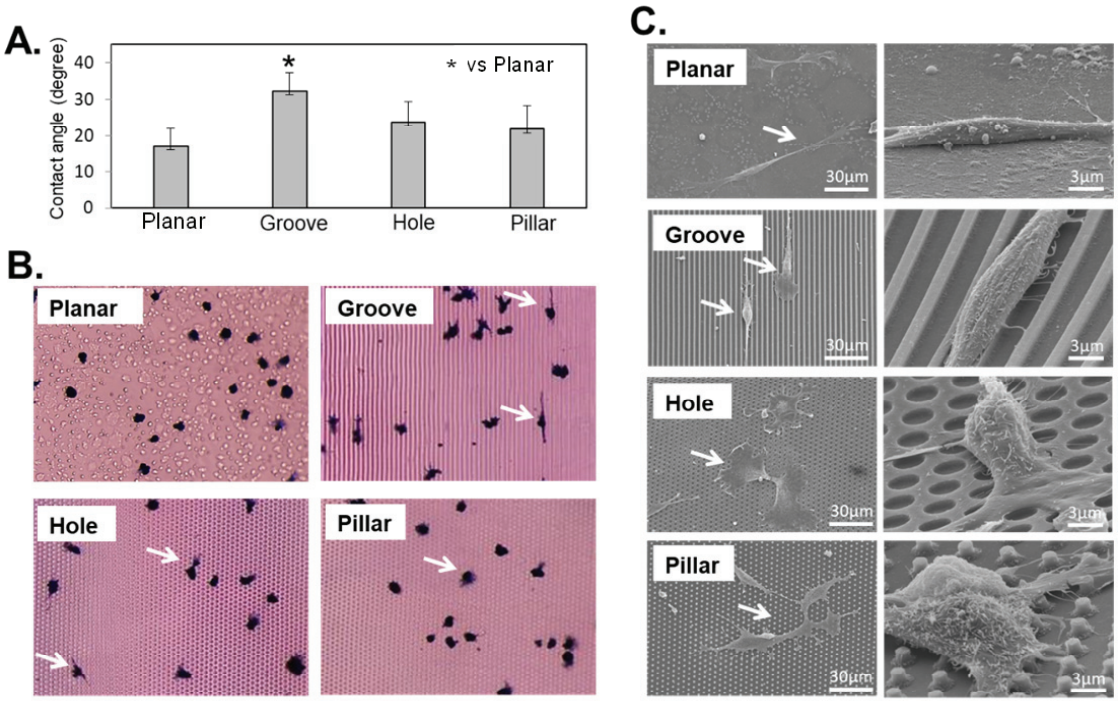

Figure 5
(A) Water contact angles on planar chitosan or patterned chitosan (2 μm in diameter and 2 μm in height). (B) Giemsa stain images of MC3T3-E1 cells attached on the planar chitosan or patterned chitosan (2 μm in diameter and 2 μm in height). The cells were incubated on the patterns for 2 h. (C) SEM images of MC3T3-E1 cells attached on the planar chitosan or chitosan pillars 2 μm in diameter and 2 μm in height. The cells were incubated on the patterns for 24 h.

diameter and width were able to be fabricated. The fine detail and sharpness of our micro/nano-patterns was similar to that of chitosan micro/nano-patterns previously reported [27,30].

2. Antibacterial activity of chitosan patterns

We estimated the effect of the shape and size of the chitosan patterns on bacterial attachment by a bacterial attachment assay using *S. mutans* incubated for 1 h on different-sized chitosan pillars and observing the morphology (Fig. 3A) and the number (Fig. 3B) of *S. mutans* attached to a chitosan planar surface and the chitosan pillars 2 μm, 1 μm, or 500 nm in diameter and 2 μm in height. Few *S. mutans* cells were observed on the tips of the pillars. The bacteria could not reach the bottom of the pillars and the spaces between pillars because these spaces were too narrow for the cells, which are ca. 1 μm to 500 nm in diameter. Interestingly, the bacteria attached weakly onto 500 nm diameter pillars but attached below and between pillars 2 μm or 1 μm in diameter. More bacteria attached onto pillars than on planar chitosan (Fig. 3B). The increase in *S. mutans* attachment due to the patterning of chitosan pillars was consistent with the increase in *Staphylococcus aureus* attachment by microgroove patterning of chitosan previously reported [31]. A similar trend in bacterial adhesion was reported for hydroxyapatite micro-patterns [32]. The bacteria are effectively captured due to surface roughness and the large surface area of the pillars. However, the observed tendencies were in contrast to the decrease in bacterial adhesion on polyurethane nano-pillars [33], suggesting that the type and size of the pattern, and the material type, are important for bacterial adhesion on patterns. Furthermore, the highest number of attached cells was observed on chitosan pillars 1 μm in diameter. The distance between these chitosan pillars would just accommodate an *S. mutans* cell, which is ca. 1 μm to 500 nm in diameter. Thus, patterns with appropriate shape and size supported stable cell attachment.

We investigated the effect of chitosan patterns on colony formation by *S. mutans* after 5 days' incubation. Figure 4A shows SEM images of *S. mutans* colonies on planar PET, glass, and chitosan, and chitosan pillars with 500 nm, 1 μm, and 2 μm diameters. Figure 4B shows the area (cm^2/cm^2) of the colonies on the samples. Colonies were randomly distributed on planar PET and glass but no colonies were observed on planar chitosan or pillars. Figure 4C shows the LIVE/DEAD bacterial viability assay results for *S. mutans* on planar glass, used as a control, and on planar chitosan, each incubated for 1 h. Green fluorescence indicates active bacteria, and red fluorescence indicates inactivated bacteria. The number of inactivated bacteria on planar chitosan was higher than on planar glass, suggesting that chitosan surfaces with or without patterns have anti-bacterial activity against *S. mutans*.

Our chitosan patterns were prepared using un-neutralized chitosan films by thermal crosslinking. Thus, the resulting acetic acid salts of the amino group of chitosan exhibited strong antibacterial activity [29]. Several antibacterial mechanisms of chitosan have been proposed [34]. The cationic nature of the protonated amino group (NH_3^+) of chitosan destroys the negatively charged cell membranes and cell walls of bacteria, resulting in cell death [20]. In our case, a small number of attached bacteria were inactivated on the chitosan surfaces, stopping *S. mutans* colony formation. The observed inhibition of *S. mutans* colony formation on our planar and pillar chitosan surfaces is similar to the decrease in colony formation by *S. aureus* on chitosan grooves [31]. Slight differences in anti-bacterial activity would depend on the bacterial species, size and shape of the chitosan patterns, and the properties of the chitosan films formed using different processes.

Interestingly, some biomimetic patterns inhibit bacterial colony formation and exhibit anti-bacterial activity [35-37]. Polydimethylsiloxane elastomer micro-patterns based on shark skin prevent the formation of bacterial biofilms [35], and nano-pillars based on cicada wings exhibit effective bactericidal activity [36]. In the future, chitosan patterns could be designed to further decrease bacterial attachment and enhance anti-bacterial surfaces.

3. Cell attachment

We investigated the effects of chitosan patterns on the elongation and spreading of MC3T3-E1 cells. The contact angle was highest for the groove pattern, suggesting that wettability decreased (Fig. 5A). Giemsa staining images showed that the patterned chitosan film allowed cell adhesion after 2 hours of incubation. In particular, the groove pattern most effectively supported cell elongation (Fig. 5B). SEM observation after 24 hours of incubation showed spindle-shaped fibroblasts on the planar and groove pattern films. In the groove patterned film, the cells aligned in the direction of the grooves and extended long cell processes along the groove. In the hole pattern, the cells were more spread out compared to the other patterns. On the pillar-patterned film, the cell processes extended through the apex of the column (Fig. 5C). These results suggest that chitosan patterns might

regulate cell adhesion and behavior, in addition to having antibacterial properties. These results are similar to those of our previous studies of cell behavior using nano/micro patterns [22,38,39]. Cell adhesion proteins, such as fibronectin, anchored on the pattern might interact with inoculated cells [40].

Conclusion

We prepared chitosan fine patterns using the imprint method and examined bacterial/cell attachment to micro-patterns comprising grooves, pillars, and holes. Many mammalian cells adhered to chitosan pillars with a diameter of 1 μm, whereas bacterial attachment was suppressed on any micropattern of chitosan. Moreover, the type of pattern was found to affect cell adhesion and morphology. Patterned chitosan films may thus be beneficial as bioactive interfaces with antibacterial and cell regulation properties.

Acknowledgments

This work was supported by JSPS KAKENHI Grant Numbers 22791916, 25463210, and 19H04461.

Conflict of interest

The authors report that they have no conflicts of interest related to this study.

References

1) Yang Y, Kim KH, Ong JL. A review on calcium phosphate coatings produced using a sputtering process-an alternative to plasma spraying. Biomaterials 2005; 26: 327-337.
2) Kwok CT, Wong PK, Cheng FT, Man HC. Characterization and corrosion behavior of hydroxyapatite coatings on Ti6Al4V fabricated by electrophoretic deposition. Appl Surf Sci 2009; 255: 6736-6744.
3) Woo KM, Chen VJ, Ma PX. Nano-fibrous scaffolding architecture selectively enhances protein adsorption contributing to cell attachment. J Biomed Mater Res A 2003; 67: 531- 537.
4) Kalita SJ, Bhardwaj A, Bhatt HA. Nanocrystalline calcium phosphate ceramics in biomedical engineering. Mater Sci Eng C 2007; 27: 441-449.
5) Ibara A, Miyaji H, Fugetsu B, Nishida E, Takita H, Tanaka S, Sugaya T, Kawanami M. Osteoconductivity and biodegradability of collagen scaffold coated with nano-β-TCP and fibroblast growth factor 2. J Nanomater 2013; 46: 1-11.
6) Murugan R, Molnar P, Rao KP, Hickman JJ. Biomaterial surface patterning of self-assembled monolayers for controlling neuronal cell behavior. Int J Biomed Eng Technol 2009; 2: 104-134.
7) Peter B, Pioletti DP, Laib S, Bujoli B, Pilet P, Janvier P, Guicheux J, Zambelli PY, Bouler JM, Gauthier O. Calcium phosphate drug delivery system: influence of local zoledronate release on bone implant osteointegration. Bone 2005; 36: 52-60.
8) Taha M, Chai F, Blanchemain N, Goube M, Martel B, Hildebrand HF. Validating the poly-cyclodextrins based local drug delivery system on plasma-sprayed hydroxyapatite coated orthopedic implant with toluidine blue O. Materials Science and Engineering: C, 2013; 33: 2639-2647.
9) Alves NM, Mano JF. Chitosan derivatives obtained by chemical modifications for biomedical and environmental applications. Int J Biol Macromol 2008; 43: 401-414.
10) Lu HH, El-Amin SF, Scott KD, Laurencin CT. Three-dimensional, bioactive, biodegradable, polymer–bioactive glass composite scaffolds with improved mechanical properties support collagen synthesis and mineralization of human osteoblast-like cells in vitro. J Biomed Mater Res A 2003; 64: 465-474.
11) Zhang M, Li XH, Gong YD, Zhao NM, Zhang XF. Properties and biocompatibility of chitosan films modified by blending with PEG. Biomaterials 2002; 23: 2641-2648.
12) He Q, Gong K, Ao Q, Ma T, Yan Y, Gong Y, Zhang X. Positive charge of chitosan retards blood coagulation on chitosan films. J Biomater Appl 2011; 27: 1032-1045.
13) Bojar W, Kucharska M, Ciach T, Koperski L, Jastrzębski Z, Szałwiński M. Bone regeneration potential of the new chitosan-based alloplastic biomaterial. J Biomater Appl 2014; 28: 1060-1068.
14) Bhattarai N, Gunn J, Zhang M. Chitosan-based hydrogels for controlled, localized drug delivery. Adv Drug Deliv Rev 2010; 62: 83-99.
15) Rabea EI, Badawy MET, Stevens CV, Smagghe G, Steurbaut W. Chitosan as antimicrobial agent: Applications and mode of action. Biomacromolecules 2003; 4: 1457-1465.
16) Raafat D, Sahl HG. Chitosan and its antimicrobial potential-a critical literature survey. Microb Biotechnol 2009; 2: 186-201.
17) Fernandez-Saiz P, Lagaron JM, Ocio MJ. Optimization of the biocide properties of chitosan for its application in the design of active films of interest in the food area. Food Hydrocoll 2009; 23: 913-921.
18) Raafat D, von Bargen K, Haas A, Sahl HG. Insights into the Mode of Action of Chitosan as an Antibacterial Compound. Appl Environ Microbiol 2008; 74: 3764-3773.
19) Másson M, Holappa J, Hjálmarsdóttir M, Rúnarsson ÓV, Nevalainen T, Järvinen T. Antimicrobial activity of piperazine derivatives of chitosan. Carbohyd Polym 2008; 74: 566-571.
20) Goy RC, Britto DD, Assis OBG. A review of the antimicrobial activity of chitosan. Polímeros 2009; 19: 241-247.

21) Akasaka T, Miyaji H, Kaga N, Yokoyama A, Abe S, Yoshida Y. Adhesion of Osteoblast-like Cells (Saos-2) on Micro-/Submicro-Patterned Apatite Scaffolds Fabricated with Apatite Cement Paste by Micro-Molding. Nano Biomed 2016; 8: 112-122.
22) Akasaka T, Miyaji H, Imamura T, Kaga N, Yokoyama A, Yoshida Y. Submicro-patterning of curable dental materials by molding methods: A screening trial, Dig. J Nanomater Bios 2017; 12: 281-292.
23) Torisawa Y, Takagi A, Nashimoto Y, Yasukawa T, Shiku H, Matsue T. A multicellular spheroid array to realize spheroid formation, culture, and viability assay on a chip. Biomaterials 2007; 28: 559-566.
24) Miyata S, Miyaji H, Kawasaki H, Yamamoto M, Nishida E, Takita H, Akasaka T, Ushijima N, Iwanaga T, Sugaya T. Antimicrobial photodynamic activity and cytocompatibility of Au25(Capt)18 clusters photoexcited by blue LED light irradiation. Int J Nanomedicine 2017; 12: 2703-2716.
25) Li F, Chen J, Chai Z, Zhang L, Xiao Y, Fang M, Ma S. Effects of a dental adhesive incorporating antibacterial monomer on the growth, adherence and membrane integrity of Streptococcus mutans. J Dent 2009; 37: 289-296.
26) Fernandez JG, Mills CA, Samitier J. Complex microstructured 3D surfaces using chitosan biopolymer. Small 2009; 5: 614-620.
27) Koo S, Ahn SJ, Zhang H, Wang JC, Yim EKF. Human Corneal Keratocyte Response to Micro- and Nano-Gratings on Chitosan and PDMS. Cel Mol Bioeng 2011; 4: 399.
28) Yu BY, Chou PH, Sun YM, Lee YT, Young TH. Topological micropatterned membranes and its effect on the morphology and growth of human mesenchymal stem cells (hMSCs). J Membr Sci 2006; 273: 31-37.
29) Nakashima T, Matsuo M, Bin Y, Nakano Y, Kobayashi T, Komemushi S, Sakagami Y. Mechanical Properties and Antibacterial Efficacy of Chitosan Films. Biocont Sci 2006; 11: 27-36.
30) Park I, Cheng J, Pisano AP, Lee ES, Jeong JH. Low temperature, low pressure nanoimprinting of chitosan as a biomaterial for bionanotechnology applications. Appl Phys Lett 2007; 90: 093902. https://doi.org/10.1063/1.2709914
31) Estevam-Alves R, Ferreira PH, Coatrini AC, Oliveira ON, Fontana CR, Mendonca CR. Femtosecond Laser Patterning of the Biopolymer Chitosan for Biofilm Formation. Int J Mol Sci 2016; 17(8): 1243. https://doi.org/10.3390/ijms17081243
32) Zhou Y, Xiao Y, Qiu Y, Yuan H, van Blitterswijk CA, Zhou X, Xu X, Bao C. Adhesion and proliferation of cells and bacteria on microchip with different surfaces microstructures. Biomed Tech 2016; 61: 475-482.
33) Xu LC, Wo Y, Meyerhoff ME, Siedlecki CA. Inhibition of bacterial adhesion and biofilm formation by dual functional textured and nitric oxide releasing surfaces. Acta Biomater 2017; 15: 53-65.
34) Rabea EI, Badawy ME, Stevens CV, Smagghe G, Steurbaut W. Chitosan as antimicrobial agent: applications and mode of action. Biomacromolecules 2003; 4: 1457-1465.
35) Chung KK, Schumacher JF, Sampson EM, Burne RA, Antonelli PJ, Brennan AB. Impact of engineered surface microtopography on biofilm formation of Staphylococcus aureus. Biointerphases 2007; 2: 89-94.
36) Ivanova EP, Hasan J, Webb HK, Truong VK, Watson GS, Watson JA, Baulin VA, Pogodin S, Wang JY, Tobin MJ, Löbbe C, Crawford RJ. Natural Bactericidal Surfaces: Mechanical Rupture of Pseudomonas aeruginosa Cells by Cicada Wings. Small 2012; 8: 2489-2494.
37) Heedy S, Marshall ME, Pineda JJ, Pearlman E, Yee AF. Synergistic antimicrobial activity of a nanopillar surface on a chitosan hydrogel. ACS Appl Bio Mater 2020; 3, 8040-8048.
38) Makita R, Akasaka T, Tamagawa S, Yoshida Y, Miyata S, Miyaji H, Sugaya T. Preparation of micro/nanopatterned gelatins crosslinked with genipin for biocompatible dental implants. Beilstein J Nanotechnol 2018; 11: 1735-1754.
39) Kaga N, Akasaka T, Horiuchi R, Yoshida Y, Yokoyama A. Adhesion of human osteoblast-like cells (Saos-2 cells) on micro/nanopatterned structures sputter-coated with titanium. Nano Biomed 2016; 8: 74-82.
40) Dewez JL, Lhoest JB, Detrait E, Berger V, Dupont-Gillain CC, Vincent LM, Schneider YJ, Bertrand P, Rouxhet PG, Adhesion of mammalian cells to polymer surfaces: from physical chemistry of surfaces to selective adhesion on defined patterns. Biomaterials 1998; 19: 1441-1445.

(Received: February 24, 2022/
Accepted: March 29, 2022)

Corresponding authors:
Hirofumi Miyaji, Ph.D
Department of Periodontology and Endodontology, Faculty of Dental Medicine,
Hokkaido University, N13 W7 Kita-ku, Sapporo 060-8586, Japan.
Tel: +81 11 706 4266, Fax: +81 11 706 4334
E-mail: miyaji@den.hokudai.ac.jp
Tsukasa Akasaka, Ph.D
Department of Biomaterials and Bioengineering, Faculty of Dental Medicine,
Hokkaido University, N13 W7 Kita-ku, Sapporo 060-8586, Japan.
Tel/Fax: +81 11 706 4250
E-mail: akasaka@den.hokudai.ac.jp